

## RHESSI/GOES OBSERVATIONS OF THE NONFLARING SUN FROM 2002 TO 2006

J. M. McTIERNAN

Space Sciences Laboratory, University of California, Berkeley, CA 94720-7450, USA; [jimm@ssl.berkeley.edu](mailto:jimm@ssl.berkeley.edu)  
Received 2008 June 13; accepted 2009 March 5; published 2009 April 30

### ABSTRACT

In this work, we obtain the temperature ( $T$ ) and emission measure (EM) for solar X-ray emission, using *RHESSI* and *GOES* data, at times for which there are no solar flares. Approximately 8700 time intervals during the *RHESSI* mission, from launch until 2006 August, are analyzed. We find that high-temperature emission, in the temperature range of 5–10 MK, is typically present during active times. When comparing temperature measurements, we find that *RHESSI* temperature measurements are consistently higher than *GOES* measurements, with smaller EM for *RHESSI*, but with values for the two instruments that are not necessarily well correlated.

*Key words:* Sun: corona – Sun: X-rays, gamma rays

### 1. INTRODUCTION

The *RHESSI* spacecraft carries nine germanium detectors which are used to observe solar X-rays and  $\gamma$ -rays in the energy range from 3 keV to approximately 17 MeV. From *RHESSI* data, we can obtain spectra with better than 1 keV FWHM energy resolution (Lin et al. 2002; Smith et al. 2002). During solar flares, *RHESSI* can detect emission from plasmas with temperatures  $\gtrsim 10$  MK. *RHESSI* can detect both the thermal continuum and line emission (from Fe and Fe/Ni line complexes).

Since *RHESSI* was launched in 2002 February, it has observed thousands of solar flares. It has also observed solar emission above 3 keV when there are no flares present. The plasma temperature required for this high-energy emission is greater than 5 MK, a temperature range that is not often considered for solar active regions (Benz & Grigis 2002).

Typically, the temperature of active regions on the Sun is given as 1–2 MK. There have been numerous studies of the solar differential emission measure (EM) in the temperature range below 5 MK (e.g., Warren & Winebarger 2003). This temperature range is dependent mostly on the instruments used for the temperature measurement (e.g., *TRACE*, *EIT*, *CDS*, *SUMER*) which have little sensitivity above 5 MK.

Older instruments have given some relatively high-temperature results for active region plasma. Data from *Sky-lab* (Dere 1982) resulted in temperature measurements of 5 MK for active regions. The *Yohkoh* BCS measured active region temperatures in the range of 2.5–4 MK (Watanabe et al. 1995). Similar temperatures have been found from data of *Yohkoh* SXT (Klimchuk & Gary 1995). Results with higher temperatures for single active regions have very recently been obtained using the *Hinode* XRT instrument (Reale et al. 2009; Schmelz et al. 2009). Note that all of these high-temperature measurements are for small samples of active region data.

In this work, we use *RHESSI* data for nonflaring times, along with *GOES* data, to determine the temperature and EM for the Sun in this high-temperature range. The time period from launch until 2006 August is examined. Note that this work is unrelated to the calculations presented by Hannah et al. (2007), who presented *RHESSI* spectra for the Sun at its quietest. For this work, the Sun is not as quiet; instead there are active regions and often a large soft X-ray component in the observed emission.

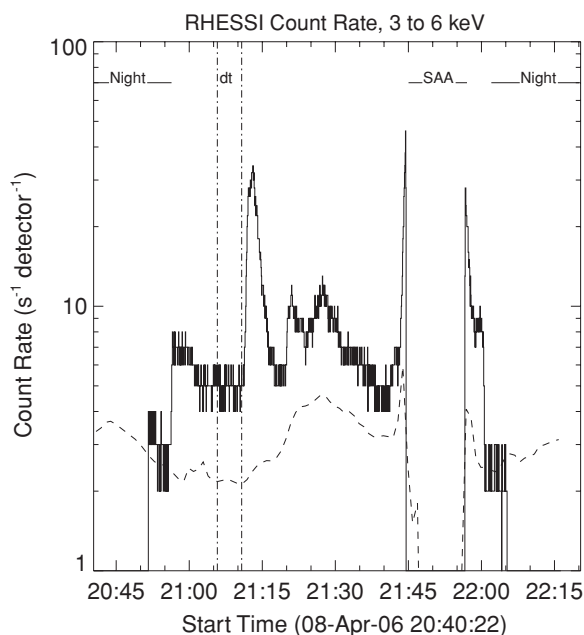
### 2. DATA INTERVAL SELECTION AND BACKGROUND SUBTRACTION

Figure 1 shows the *RHESSI* 3–6 keV count rate for one spacecraft orbit. The orbit time range is chosen so that it starts and ends during spacecraft night; time ranges for spacecraft night are marked near the top of the plot. Except for 5 minute periods before and after the day–night transitions, the front detector segments are turned off at night and the count rate is zero. The gap in the data starting at approximately 21:45 UT is due to the detectors being turned off as the spacecraft passes through the South Atlantic Anomaly (SAA).

As the spacecraft passes through the day–night boundary, there is a change in the count rate; the rate jumps as the spacecraft passes from night to day at approximately 20:51 UT, and there is a corresponding decrease as the spacecraft passes back from day to night at approximately 22:02 UT. The count rate during spacecraft daytime is always higher than that immediately before and after, independent of any flaring activity; this excess is clearly solar emission. This is typically true when there are active regions visible on the solar disk. The estimated background level, based on the position of the spacecraft as will be explained shortly, is shown on the plot as a dashed line.

The vertical dashed lines in Figure 1, plotted at 21:06 and 21:11 UT, show an interval which was chosen for a temperature measurement. The time intervals used in this study are chosen for their lack of flare (or microflare) emission. For each orbit, an interval of between 1 and 5 minutes was chosen based on the following criteria: no flares or particle events were allowed in the intervals, both the thick and thin attenuators were in the “out” position, no data gaps were allowed, and each interval was at least 5 minutes from the SAA. The intervals chosen have the minimum (daylight) count rate for the orbit, subject to a flatness test. To insure a flat count rate, thus avoiding microflares, the dispersion of the count rate for an interval was required to be less than 1.25 times the dispersion expected from a Poisson distribution.

The background level represented by the count rates just before and after spacecraft day is not necessarily a constant throughout the orbit. It is dependent on the cosmic ray flux and local particle flux, and it varies with the position of the spacecraft. Figure 2 shows the background count rate in the 3–6 keV energy band for the *RHESSI* detectors that will be used in this calculation, averaged over the whole mission. Here, the



**Figure 1.** *RHESSI* 3–6 keV count rate for one *RHESSI* orbit, on 2006 April 8, from 20:40:20 UT to 22:16:20 UT. Intervals for spacecraft night, SAA passage, and  $T$  measurement are indicated on the plot.

background level is plotted versus the longitude of the ascending node of the orbit and the orbital phase. The longitude of the ascending node is the longitude at which the spacecraft passes over the equator, moving from south to north; the combination of this quantity and the orbital phase gives complete information about the latitude and longitude of the spacecraft. On orbit, a spacecraft follows a series of vertical lines on this plot, going up. The spacecraft position for the time period of the plot shown as Figure 1 is shown as a series of + signs on Figure 2.

The background level was obtained in the following manner. The count rate has been accumulated in 20 s intervals during the 5 minute periods before and after daylight for each orbit in the mission. This resulted in approximately 500,000 spectra. Each of these spectra has an energy range from 3 to 300 keV. This energy range is split into 492 energy bands with 1/3 keV resolution from 3 to 100 keV and 1 keV resolution from 100 to 300 keV.

The spectra are then averaged over time, longitude of the ascending node, and orbital phase. The angular ranges are split into  $10^\circ$  bins. It takes a relatively long time for all of the possible angular combinations to be visited by the spacecraft; it turns out that a 56 day time interval is sufficient to ensure that there are measurements in each angular bin. For each of the 56 day time intervals, the individual spectra in each angular bin are averaged, resulting in a  $36 \times 36$  array, similar to the image plotted in Figure 2, for each of the 492 energy bands. We end up with an array of  $492 \times 18 \times 36 \times 36$  for each 56 day interval; 492 energy bands, 18 detector segments, 36 bins of ascending node longitude, and 36 bins of orbital phase. Each of these arrays is stored in an IDL save file.

To calculate a background spectrum for a given time from this database, we restore the files accumulated for times that bracket the given time, and interpolate the spectrum over time and position. This can be done for any time or energy band for the whole *RHESSI* mission.

The uncertainty in the background is the dispersion obtained in each of the  $36 \times 36$  angular bins during the averaging process,

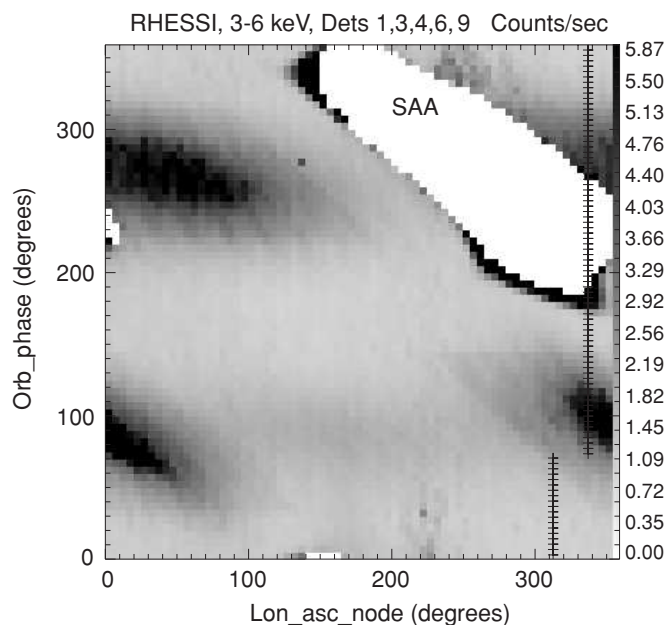


**Figure 2.** Background level for *RHESSI* 3–6 keV count rate, averaged for the full mission, plotted vs. the longitude of the ascending node of the orbit and orbital phase. The path of the spacecraft is denoted by + signs. The scale on the right-hand side refers to the background count rates shown on the image. The white area on the upper right is the South Atlantic Anomaly.

For the low-latitude regions where most of the temperature measurements were taken, the uncertainty in the background is approximately 1/2 the background rate. For the 3–6 keV energy band shown in Figure 1, this is approximately 1 count per second per detector. The uncertainty is higher for higher latitude regions (e.g., regions that are very dark in Figure 2).

### 3. TEMPERATURE MEASUREMENTS

A total of 8747 time intervals were analyzed, from 2002 February 14 to 2006 August 2. Of these intervals, 6961 had enough counts above the background level in the  $>3$  keV energy range for an isothermal spectrum to be fitted, resulting in temperature and EM values for *RHESSI*. The spectra for the fits were accumulated in 1/3 keV energy channels in the energy range from 3 to 30 keV. To be included in the fit, the background-subtracted count rate for a channel was required to be greater than three times its uncertainty. Five of the nine *RHESSI* front segment detectors (detectors 1, 3, 4, 6, and 9) were used for this calculation; of the others, three (detectors 2, 5, and 7) have degraded energy resolution at low energies, and one (detector 8) has occasional interference from one of the spacecraft transmitters. The *RHESSI* spectra were fitted using the SSW XRAY package which (via `chianti_kev.pro`) uses version 5.2 of the Chianti database (Landi et al. 2006).

We also obtained temperature and EM for each interval from *GOES* data. *GOES* 10 data were used prior to 2003 March 16, and *GOES* 12 data were used after. The *GOES*  $T$  and EM were obtained from the ratio of the data in the two channels, using the results of White et al. (2005). Coronal abundances were assumed for both the *GOES* and *RHESSI* analyses. Note that this calculation has also been performed using photospheric abundances. The results differ systematically, but differently for *GOES* and *RHESSI*. For *GOES*, the temperature assuming photospheric abundance is  $0.67 \pm 0.23$  MK lower than found for coronal abundance. For *RHESSI*, the abundance change has

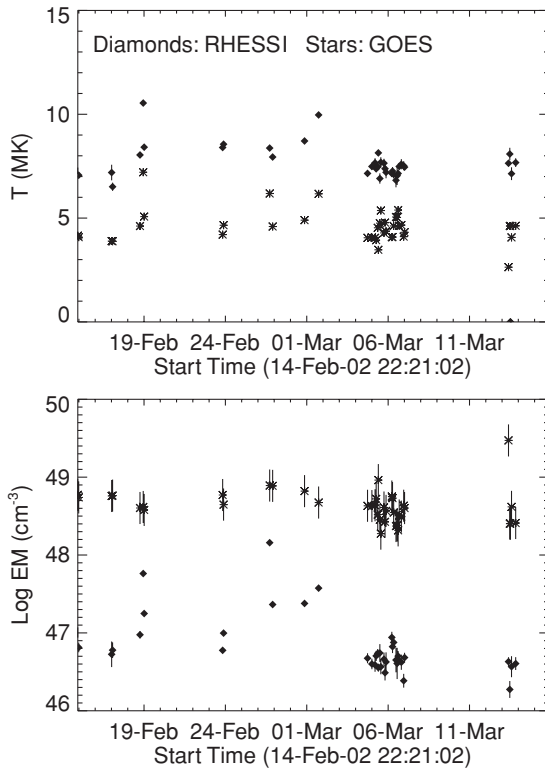


**Figure 3.** Temperature and emission measure for *GOES* (stars) and *RHESSI* (diamonds) for all suitable intervals during the first 28 days of the *RHESSI* mission.

a smaller effect, the  $T$  measured using photospheric abundance is  $0.13 \pm 0.33$  MK higher than found for coronal abundance.

Figure 3 shows temperature (in MK) and EM (in  $\text{cm}^{-3}$ ) for *RHESSI* and *GOES* for (approximately) the first month of the mission. The differences between the *GOES* and *RHESSI*  $T$  and EM values are significant. The *RHESSI* temperature is between 6 and 11 MK, and the *GOES* temperature is between 3 and 6 MK. This is generally true early in the mission. The *GOES* EM is typically a factor of 50–100 times the *RHESSI* EM. This is consistent with a differential EM that decreases with increasing temperature. The uncertainties in the *RHESSI* measurements are calculated using the assumption that the uncertainties in the count rates are Poisson distributed.  $3\sigma$  error bars are actually plotted on the figure, but the values are mostly smaller than the symbols used to denote the  $T$  and EM values; the uncertainty in  $T$  is typically less than 0.1 MK and the uncertainty in EM is typically less than  $1.0 \times 10^{46} \text{ cm}^{-3}$ . For the *GOES* measurements, the uncertainties are based on values given by Garcia (1994); 15.8% for the long-wavelength *GOES* channel and 13.8% for the short-wavelength *GOES* channel. These values typically result in uncertainties of less than 0.1 MK in  $T$  and a few times  $10^{48} \text{ cm}^{-3}$  in EM.

The *GOES* and *RHESSI* values show correlation early in the mission, but there is some scatter. A plot of the *GOES* versus *RHESSI* measurements for the first seven months of the mission (until 2002 September 14) is shown in Figure 4; for this sample, the correlation coefficient between the two values of  $T$  is 0.61. For EM it is 0.29. A best-fit regression line is shown as a dash-dotted line on the plot. This line has a slope of 0.89. There is no a priori reason to expect that the two temperature measurements will be well correlated, since *RHESSI* and *GOES* observe different temperature ranges.

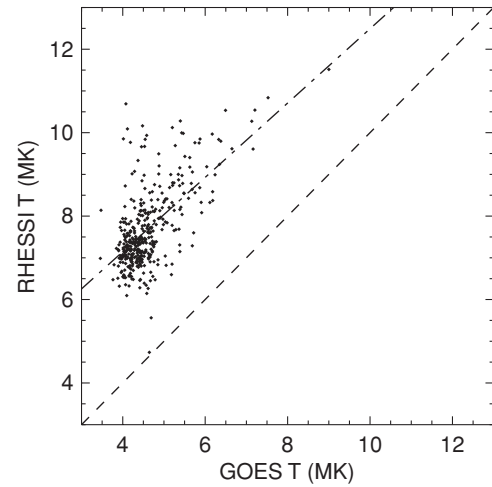


**Figure 4.** *RHESSI* temperature vs. *GOES* temperature for time intervals up to 2002 September 14. The dash-dotted line is a linear fit with slope of 0.89. The dashed line indicates where the two temperatures are equal.

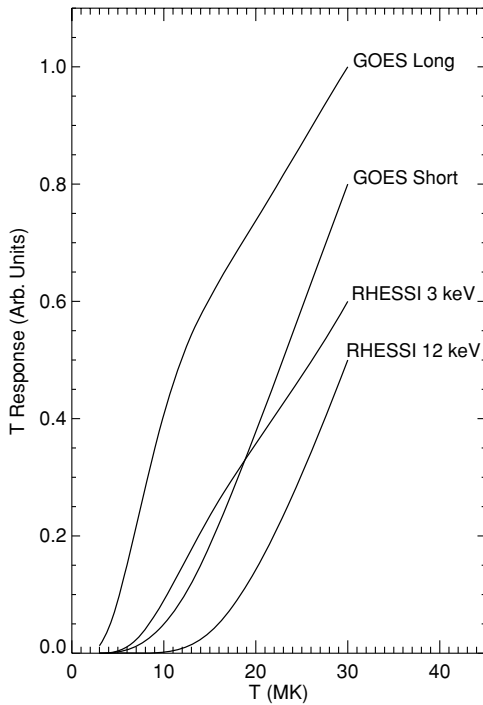
We do expect, however, that for any given time interval the *GOES* temperature will be lower than the *RHESSI* temperature. As seen in Figure 4 this is the case for the early part of the mission. We expect this because the *GOES* detector response extends to a lower X-ray energy (8 Å or 1.5 keV) than for *RHESSI* (3 keV). Figure 5 shows a plot of the temperature responses used for the two *GOES* channels, and for selected *RHESSI* energy bands. Here, it is seen that *GOES* is much more responsive to lower temperature plasma (in the 3–5 MK range) that *RHESSI* does not see. If we make the reasonable assumption that the Sun has an EM distribution that varies with temperature, then the measured average value of the  $T$  will be lower for *GOES*. The correlation between the two measurements, however, will depend on the slope of the EM distribution, and there is no reason to expect that this is not variable, which is why we should not expect that the correlation will be absolute.

This relationship between *GOES* and *RHESSI* does not hold for the full mission. Figure 6 shows the temperature comparison plot for the full mission. There are many intervals for which the *GOES* temperature is greater than the *RHESSI* temperature and there is no apparent correlation between the two measurements from late 2002 on.

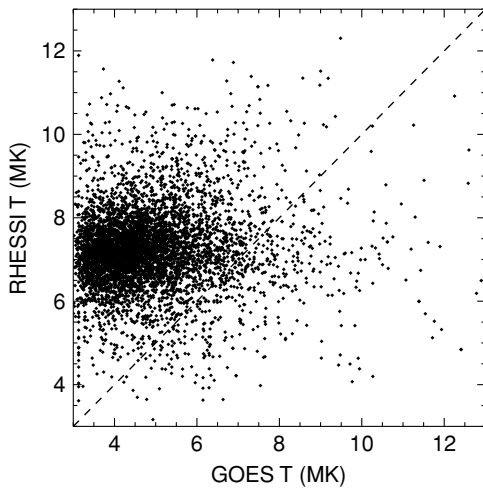
#### 4. LONG-TERM VARIATIONS

Figure 7 shows the variation of the temperature and EM for the *RHESSI* mission. The top plot shows 28 day averages of the *RHESSI* (diamonds) and *GOES* (stars) temperature. The middle plot shows the EM. The averages do not include intervals for which there was not enough emission for temperature measurements. The bottom plot shows the relative fraction of intervals for which there were no good measurements for *RHESSI*. The dashed line is the normalized average sunspot number, which we use as a measure of overall solar activity. As activity decreases, the likelihood for good measurements decreases.

The average *RHESSI* temperature is relatively constant for the mission, with a very slight drop from the 7–8 MK range to the 6.5–7.5 MK range. The *RHESSI* EM bounces up and down, but the bounces are superposed on a steady decrease of about 1 order of magnitude. Some of the bounces are pretty well correlated with the monthly sunspot number, particularly



**Figure 5.** Temperature response curves for the two *GOES* channels and two selected *RHESSI* energies.



**Figure 6.** *RHESSI* temperature vs. *GOES* temperature for all time intervals. The dashed line indicates where the two temperatures are equal.

in 2002; the correlation coefficient between *RHESSI* EM and sunspot number is 0.61. The *GOES* values start relatively constant, and then become erratic at the start of 2003 (the average *GOES T* does remain lower than the average *RHESSI T*). *GOES T* does not correlate well with sunspot number, but the *GOES* EM decreases steadily.

There is still the issue with the unexpected presence of *GOES* measurements with higher *T* than *RHESSI* measurements. We believe that this is due to the fact that the *GOES* measurements do not include background subtraction. There is no “spacecraft night” for *GOES*, and there is no way to separate nonsolar background from solar emission. The *GOES* measurements are affected by the presence of charged particles (Garcia 1994) and the relative effect of the particles increases as solar emission decreases. After 2002, it may be that the nonflare solar emission is not large enough to dominate over background effects.

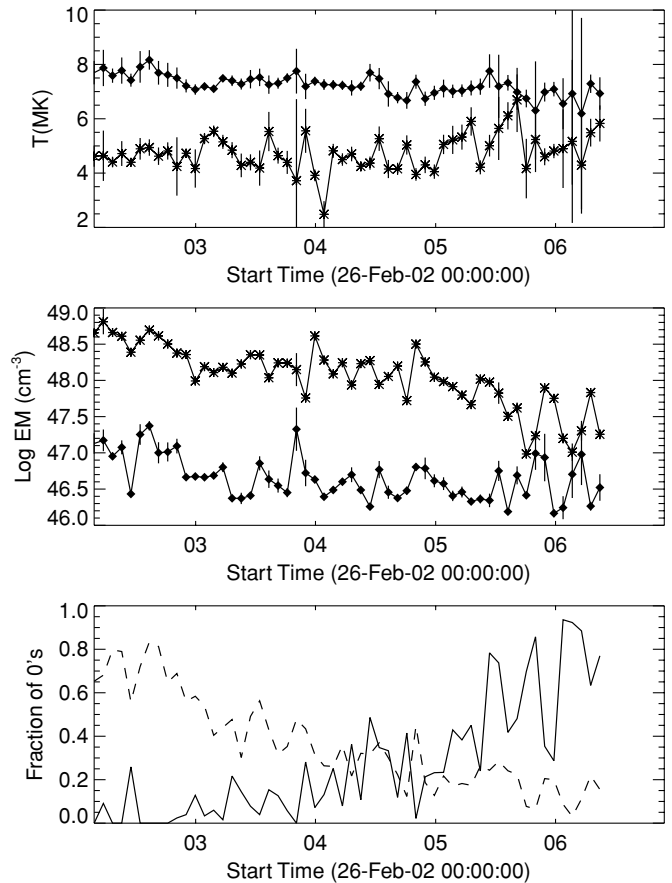


**Figure 7.** Top: 28 day averages of *GOES* (stars) and *RHESSI* (diamonds) *T*. Middle: 28 day averages of *GOES* (stars) and *RHESSI* (diamonds) EM. Bottom: the solid line is the fraction of time intervals that resulted in zero value for *RHESSI* temperature. The dashed line is a normalized value of sunspot number.

We can estimate the level at which *GOES T* and EM measurements begin to become affected by checking the frequency of intervals for which the *GOES T* is higher than the *RHESSI T*. The top panel of Figure 8 shows the fraction of measurements for which the *GOES T* is higher plotted for 28 day time intervals as a function of time. This fraction is zero for a few months of 2002, but often becomes fairly large late in the mission. The bottom panel shows this fraction plotted versus average *GOES* EM for all of the 28 day time periods. Although there are some time periods for which the fraction is zero for low *GOES* EM, the fraction is sure to be zero for EM greater than  $3 \times 10^{48} \text{ cm}^{-3}$ . This corresponds to a flux of approximately  $1 \times 10^{-6} \text{ W m}^{-2}$ , or *C* level in the short-wavelength *GOES* channel. So below *C* level, we believe that the nonbackground-subtracted *GOES* measurements may be problematic, and users should take extreme care when interpreting these results. Note that this is not an issue for flare studies, which constitute the vast majority of *GOES* data analyses. Valid *T* and EM values can always be obtained for flares as long as the appropriate preflare background is subtracted.

### 5. DISCUSSION

Regardless of the difficulties involved in the *RHESSI*–*GOES* comparison, we still have shown that there exists 5–10 MK emission from the Sun, in the absence of solar flares, which has not been previously well documented. The best-known “heating mechanism” for high-temperature loops in active regions is the

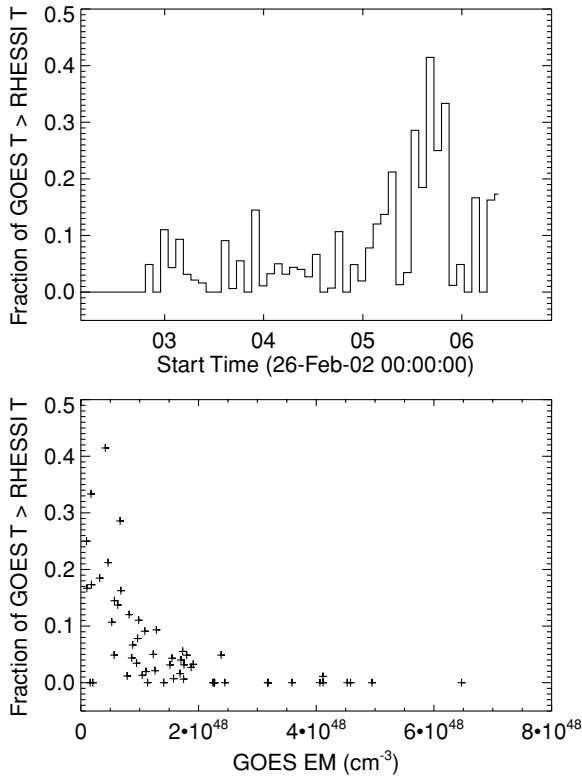


**Figure 8.** Top: the fraction of measurements for which *GOES T* was greater than *RHESSI T* (taking uncertainties into account) accumulated over 28 day intervals for the *RHESSI* mission. Bottom: same fraction vs. *GOES EM*.

heating by flares of postflare loops. It is possible that the high-temperature component observed here is due to plasma that was heated in flares or microflares. This was the conclusion reached by Watanabe et al. (1995) for the 2.5–5 MK emission observed by *Yohkoh* BCS. The high-temperature component in active region emission could also be due to heating by nanoflares (Klimchuk et al. 2007).

Figure 9 is a plot of the *RHESSI* EM for each time interval versus the time elapsed since the most recent *GOES* flare. If flares are primarily responsible for the high  $T$  emission, we would expect some correlation between this time and the amount of emission. The emission should decrease as the time since the last flare increases. There is a hint of correlation in that most of the highest values of EM ( $\gtrsim 3 \times 10^{47} \text{ cm}^{-3}$ ) are within the first 60 minutes after a flare. There is no significant correlation in the full sample, though the correlation coefficient between elapsed time and EM is  $-0.04$ . (The calculation only considered the previous day's flares, so the points at 1440 minutes are lower limits.) In many cases, the high-temperature EM persists for hours after a flare.

Can an impulsively heated coronal loop last for hours without extra heating? Using the CHIANTI package (Landi et al. 2006), we estimate the radiative cooling time for an impulsively heated loop with a density of  $n = 10^9 \text{ cm}^{-3}$  and a temperature of 8 MK to be approximately 200 minutes. It is possible that cooling can happen conductively and the conductive cooling time can be shorter than radiative cooling time. We estimate the conductive cooling time by  $\tau_c = 1.5 \times 10^{-9} n L^2 / T^{5/2}$ , where  $n$  is the plasma density and  $L$  is the loop half-length in cm. For this case, if we assume a loop length of  $10^5 \text{ km}$ , then the conductive cooling time is approximately 13 minutes. Cargill et al. (1995) showed that the overall cooling time can be approximated by a

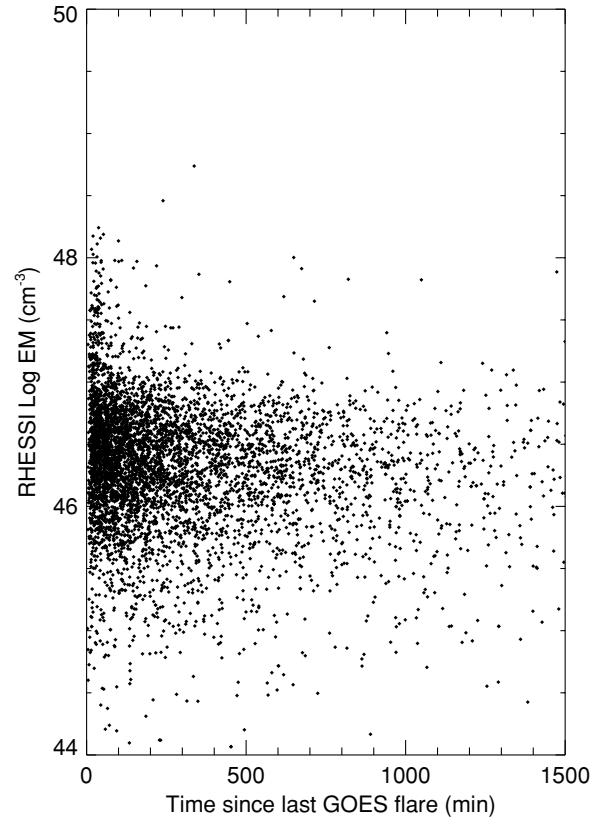


**Figure 9.** Top: the *RHESSI* emission measure, plotted for each time interval vs. the time since the most recent *GOES* flare.

combination of the conductive and radiative cooling times, given by  $\tau_{\text{mix}} = (5/3)\tau_r^{7/12} * \tau_c^{5/12}$ . If we adopt this expression, then the expected cooling time is approximately 64 minutes. This would imply that intervals with longer times since the most recent flare would need some additional heat source.

There are, in fact, smaller events, not in the *GOES* event list, that may heat the plasma. *RHESSI* has shown that microflares are extremely common—anywhere from 5 to 90 flares per day (Christe et al. 2008). Unfortunately, we cannot use the *RHESSI* microflare list for this calculation due to large gaps in the microflare data due to spacecraft night, SAA passage, and attenuators. It is entirely possible, however, that every interval is less than an hour after a microflare. Whether a single small microflare can result in enough heat to result in a persistent EM as large as observed is an issue that is beyond the scope of this work, but has been addressed by solar heating experts (see, for example, Klimchuk et al. 2007).

## 6. CONCLUSIONS

In summary, we find that high-temperature solar emission (greater than 5 MK) is usually present without flares, and is observed by *RHESSI*. The average *RHESSI* temperature ranges from 6 to 8 MK, with EMs from  $10^{46}$  to  $10^{47} \text{ cm}^{-3}$ . Individual measurements may have higher temperature and EM, ranging up to 11 MK and  $10^{48} \text{ cm}^{-3}$ . The average *GOES* temperature is 4–6 MK, consistently less than the *RHESSI* temperature, but due to the lack of background subtraction for the *GOES* data, we have some concerns regarding the use of these data when the EM is smaller than  $3 \times 10^{48} \text{ cm}^{-3}$ . The relative number of successful high-temperature measurements decreases with solar

activity. The high-temperature emission shows some variation with the solar cycle in both  $T$  and EM.

The author thanks J. Klimchuk and S. Patsourakos for useful discussions. This work was supported by NASA contract NAS5-98033 and NASA grant NNX08AJ18G.

#### REFERENCES

- Benz, A. O., & Grigis, P. C. 2002, *Sol. Phys.*, 210, 431  
Cargill, P. J., Mariska, J. T., & Antiochos, S. K. 1995, *ApJ*, 439, 1034  
Christe, S., Hannah, I. G., Krucker, S., McTiernan, J., & Lin, R. P. 2008, *ApJ*, 677, 1385  
Dere, K. P. 1982, *Sol. Phys.*, 77, 77  
Garcia, H. A. 1994, *Sol. Phys.*, 154, 275  
Hannah, I. G., Hurford, G. J., Hudson, H. S., Lin, R. P., & van Bibber, K. 2007, *ApJ*, 659, L77  
Klimchuk, J. A., & Gary, D. E. 1995, *ApJ*, 448, 925  
Klimchuk, J. A., Patsourakos, S., & Cargill, P. J. 2007, *ApJ*, 682, 1351  
Landi, et al. 2006, *ApJS*, 162, 261  
Lin, R. P., et al. 2002, *Sol. Phys.*, 210, 3  
Reale, F., Testa, P., Klimchuk, J. A., & Parenti, S. 2009, *ApJ*, in press  
Schmelz, J. T., Saar, S. H., Deluca, E. E., Golub, L., Kashyap, V. L., Weber, M. A., & Klimchuk, J. A. 2009, *ApJL*, in press  
Smith, D. M., et al. 2002, *Sol. Phys.*, 210, 33  
Warren, H. P., & Winebarger, A. R. 2003, *ApJ*, 596, L113  
Watanabe, T., et al. 1995, *Sol. Phys.*, 157, 159  
White, S. M., Thomas, R. J., & Schwartz, R. A. 2005, *Sol. Phys.*, 227, 231